

Cite this: *Phys. Chem. Chem. Phys.*, 2011, **13**, 8433–8440

www.rsc.org/pccp

PAPER

Dynamics of H and D abstraction in the reaction of Cl atom with butane-1,1,1,4,4,4-d₆

Armando D. Estillore, Laura M. Visger-Kiefer, Tarek Abdul Ghani and Arthur G. Suits*

Received 15th January 2011, Accepted 26th January 2011

DOI: 10.1039/c1cp20137a

We report the primary (D-atom) and secondary (H-atom) abstraction dynamics of chlorine atom reaction with butane-1,1,1,4,4,4-d₆. The H- and D-atom abstraction channels were studied over a range of collision energies: 10.4 kcal mol⁻¹ and 12.9 kcal mol⁻¹; 5.2 kcal mol⁻¹ to 12.8 kcal mol⁻¹, respectively, using crossed molecular beam dc slice ion imaging techniques. Single photon ionization at 157 nm was used to probe the butyl radical products resulting from the H- and D-atom abstraction reactions. These two channels manifest distinct dynamics principally in the translational energy distributions, while the angular distributions are remarkably similar. The reduced translational energy distribution for the primary abstraction showed marked variation with collision energy in the backward direction, while the secondary abstraction showed this variation in the forward direction.

Introduction

The insights obtained from the many dynamical studies on the interaction of free radicals with hydrocarbons^{1–9} (RH) has helped build a foundation for understanding the processes involved in combustion, atmospheric, and marine environments. However, in fundamental studies involving polyatomic reactants and polyatomic products, both experimentalists and theoreticians are faced with challenging dynamical issues. Polyatomic reactants may have multiple reaction sites that can exhibit distinct reactive behavior. For example, H-atom abstraction from RH with three or more carbon atoms are complicated by the nature of H-atom type being abstracted, *i.e.* competing primary, secondary, or tertiary H-atoms may be present with different energetics and distinct products. Despite long interest in these questions, little direct probing of these dynamics has been achieved, and the quantity of speculation in the literature perhaps exceeds that of concrete evidence. Crossed-beam imaging methods have now developed to the point that these issues can be addressed more directly, and this paper represents the first of our efforts on this problem.

The dynamics associated with the abstraction at the different H atom sites in alkanes was studied in a widely cited set of papers of Andresen and Luntz¹ on the reaction of O(³P) with neopentane, cyclohexane, and isobutane. These were chosen as prototype systems for study of abstraction of primary, secondary, and tertiary hydrogens, respectively. This crossed-beam study relied on laser-induced fluorescence to

probe the OH product state distributions, but without translational energy or differential cross section determinations. Interestingly, in all systems the OH rotational distributions were found to be cold and they this ascribed to a collinear O–H–C transition state with low impact parameter collisions. The OH vibrational distributions, however, showed a dependence on the type of H-atom abstracted, with increasing vibrational excitation for primary, secondary and tertiary hydrogen atoms. This trend was attributed to the increasing exoergicity in this sequence, and the movement of the reaction barrier toward the reactant geometries. These findings were confirmed in the quasiclassical trajectory calculations by Luntz and Andresen.²

There have been several studies on site-selective hydrogen atom abstraction by Cl atoms from RH with three or more carbon atoms, obtained using various kinetic techniques.^{10–12} Tyndall *et al.*¹² used relative rate technique to quantify the contributions of primary and secondary H-atoms in the reaction of Cl atoms with propane and butane. They found room temperature reaction of Cl atoms with C₃H₈ yields 43 ± 3% 1-propyl and 57 ± 3% 2-propyl radicals, while the reaction of Cl + n-C₄H₁₀ produces 29 ± 2% and 71 ± 2% for abstraction of primary and secondary hydrogen atoms, respectively. Sarzynski and Sztuba¹¹ in their study of Cl + butane using the relative rate method reported a slightly positive temperature dependence for abstraction of primary hydrogen atom and slightly negative for secondary hydrogen abstraction, suggesting small barriers for the former reactions.

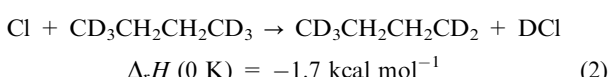
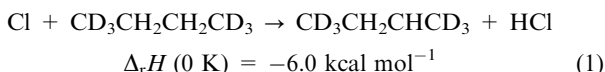
In addition to many kinetics studies, the reaction dynamics of chlorine atoms with hydrocarbons have also been studied in great detail in the past two decades. In contrast to

Department of Chemistry, Wayne State University, Detroit, Michigan 48202, USA. E-mail: asuits@chem.wayne.edu

$O(^3P) + RH$ reactions, these reactions have little or no barriers to reaction and are exoergic, with the exception of $Cl +$ methane with $\Delta H = +1.82$ kcal mol⁻¹. Zare and coworkers^{4–7,13} and Varley and Dagdigian¹⁴ investigated the dynamics of chlorine atom reactions with small hydrocarbons and their deuterated analogues using PHOTOLOC with core extraction techniques combined with resonance-enhanced multiphoton ionization (REMPI) to probe the nascent HCl (DCl) product. Results showed cold HCl and DCl rotational distributions. An earlier report on the secondary abstraction reaction of $Cl + c-C_6D_{12}$ using diode laser absorption technique also showed cold DCl rotation distributions.³ These cold HCl(DCl) rotational distributions have been exhibited by Cl atom reaction in a wide range of target alkane reactants.^{9,15} The most direct investigation involving the site-specific dynamics of $Cl + RH$ reaction was by Koplitz and co-workers¹⁶ using selectively deuterated propane. They found that the yield of DCl is nearly equal for either primary and secondary labeled propane while the HCl yield was ~1.5 times greater for $CH_3D_2CH_3$ than $CD_3CH_2CD_3$. Varley and Dagdigian^{17,18} extended this study to a PHOTOLOC investigation of partially deuterated propane and isobutane deuterated on the tertiary carbon. For the $Cl + CD_3CH_2CD_3$ reaction, results suggested sideways scattered DCl product while the HCl peaked in the backward direction. For $Cl + (CH_3)_3CD$, the nascent DCl product was mainly backscattered, suggesting that abstraction of a tertiary hydrogen atom proceeds through a near collinear transition state. Abstraction of the primary hydrogen to yield the HCl product was sideways peaked in qualitative agreement to the primary abstraction in the $Cl +$ partially deuterated propane system.

Numerous studies have demonstrated the efficiency of crossed molecular beam ion imaging techniques in providing detailed information on the dynamics of many bimolecular reactions. This technique has also been exploited in studying the dynamical consequence of isotope effects on several systems. Using crossed molecular beam ion velocity imaging techniques, Liu and coworkers¹⁹ studied reaction of Cl with CHD_3 to examine vibrational mode selectivity in that system. They found that CH stretch excitation was no more effective than translation in promoting reaction. Despite the number of studies on deuterated methane and ethane and on the dynamics of Cl atom reaction with fully hydrogenated systems, there have been no studies yet bringing the power of imaging methods to explore the dynamics of H vs. D abstraction in selectively deuterated alkanes.

In this paper, we report the reaction of chlorine atoms with butane-1,1,1,4,4,4-d₆ using crossed molecular beams and dc slice imaging techniques. In this reaction, the Cl beam crosses the partially deuterated butane beam and H- or D-atom abstraction occurs forming HCl (1) or DCl (2) and a butyl radical:



The reaction enthalpies used here are from our *ab initio* calculations using the GAUSSIAN 09²⁰ suite of software at the CBS-QB3^{21,22} level corrected for zero point energy. The butyl radical products resulting from the H-atom and D-atom abstraction were probed *via* single photon ionization using a 157 nm excimer laser. Previous results from our group have shown improved detection and sensitivity of single photon ionization in probing the dynamics of a variety of reactions.^{23,24} The key issue we wish to address here is to compare the dynamics of abstraction at the primary to that of the secondary carbon sites.

Experiment

The experiments were performed in a crossed beam imaging apparatus described elsewhere.^{25,26} The apparatus is partitioned into a main scattering chamber and two source chambers differentially evacuated to $\sim 10^{-7}$ Torr base pressure and $\sim 10^{-5}$ Torr operational pressure by turbomolecular pumps. The Cl atom beam was then generated by photodissociation of tetrachloroethylene, TCE, 5% seeded in Helium, using the 193 nm output of an ArF excimer laser (60 mJ, 10 Hz) at the nozzle of a piezoelectric pulsed valve. The Cl atom product was entrained in the beam, which was skimmed before traveling into the interaction region. Butane-1,1,1,4,4,4-d₆ (98% D, Isotec Inc.) seeded 5% in Ar, He, or H₂, was expanded from a total pressure of 4 bar through another pulsed valve, collimated by a single skimmer, and crossed the Cl beam at 90° in the interaction region. Recent measurements in our laboratory²⁷ show that photodissociation of TCE gives ~30% spin-orbit excited Cl atoms at 202 nm, and we expect a similar yield at 193 nm, as it is the same absorption band. However, we anticipate efficient quenching to the ground state during the expansion as we have seen in similar experiments with oxaly chloride as the Cl atom precursor.

The scattered butyl radical products resulting from H- or D-atom abstraction with $m/z = 63$ or $m/z = 62$, respectively, were detected by single photon ionization. Ionization of the products was achieved by a 157 nm F₂ excimer laser (OPTEX, ~0.5 mJ, 10 Hz) focused loosely using a MgF₂ lens ($f = 135$ cm) into the interaction region of the two crossed beams. Although the primary butyl radical products nominally possess an ionization energy slightly higher than the secondary radical, and slightly above the 7.9 eV probe photon energy, we have found essentially identical detection efficiencies for these two products and 157 nm, and no evidence of a dependence on internal energy.²⁸ The ions were accelerated perpendicular to the plane formed by the molecular beams *via* a four-electrode dc slice ion optics assembly²⁹ to impact on a 75 mm diameter dual microchannel plate (MCP) detector coupled to a fast phosphor screen held at 5 kV (Photonis/Burle, Sturbridge, MA). The front of the MCP assembly was held at ground potential and the back plate was pulsed to “gate” the central slice of the reaction products at a specific mass by application of a high voltage pulse (+2.2 kV/+1 kV bias, 100 ns width) using a commercial pulser (DEI PVX-4140, Fort Collins, CO). The timing of the pulsed molecular beam nozzles, firing of the photolysis and

probe lasers, and detector gate pulse were controlled using a delay generator (BNC 555, San Rafael, CA). The resulting image was recorded using a charged coupled device (CCD) camera (Mintron 2821e, 512 × 480 pixels, Taipei, Taiwan) and transferred to a computer for analysis. The dc slice imaging detection scheme, centroiding and megapixel acquisition program IMACQ were used to accumulate the raw images.³⁰ Image accumulation to reach a satisfactory signal to noise ratio took 1–3 h at a given collision energy. The conditions of a typical experiment are illustrated in an accompanying video shown in our previous publication.²³

Results

Crossed-beam scattering with single photon ionization has shown to be a sensitive approach to investigating many complex bimolecular processes.^{8,23–25,31–36} With the use of 157 nm excimer laser as our probe, partially deuterated butyl radicals formed from the H- and D-atom abstraction from Cl+ butane-*d*₆ reaction can be examined selectively. Here, we studied the H-abstraction reaction at nominal collision energies 10.4 kcal mol⁻¹ and 12.9 kcal mol⁻¹ and D-atom abstraction at three different collision energies ranging from 5.2 kcal mol⁻¹ to 12.8 kcal mol⁻¹. The spread in the collision energy is roughly 25% full-width half maximum. We do not report the image obtained in the H-abstraction at the lowest

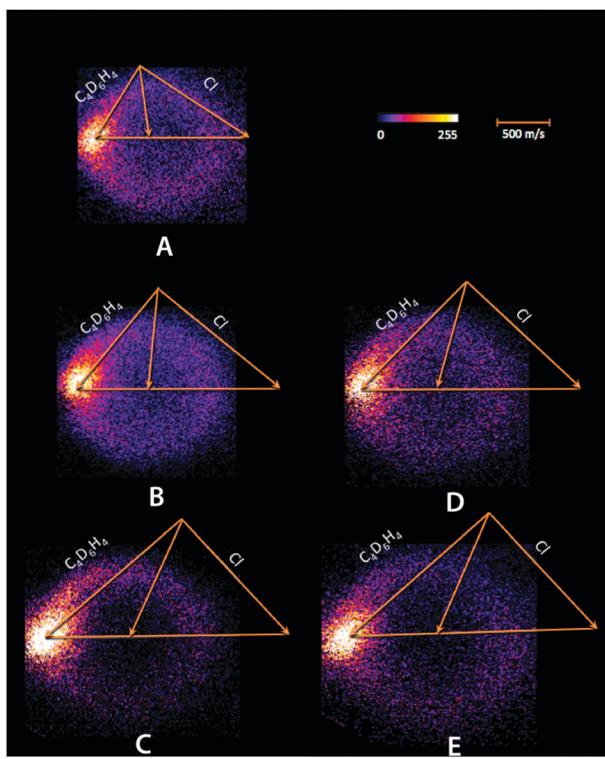


Fig. 1 DC sliced images for butyl radical resulting from the H- and D-atom abstraction from Cl atom reaction with butane-1,1,1,4,4-*d*₆ and superimposed Newton diagrams. Left panel are results from D-atom abstraction; (a) collision energy 5.2 kcal mol⁻¹; (b) collision energy 9.1 kcal mol⁻¹; (c) collision energy 12.8 kcal mol⁻¹. Right Panel are results from H-atom abstraction; (d) collision energy 10.4 kcal mol⁻¹; (e) collision energy 12.9 kcal mol⁻¹.

collision energy owing to interfering background in the backward hemisphere of the image.

Fig. 1 shows the DC sliced images of the butyl radical products from both H and D abstraction of butane deuterated at the terminal carbons, with the nominal Newton diagrams superimposed on the images. These are after background subtraction and density-to-flux correction as described fully

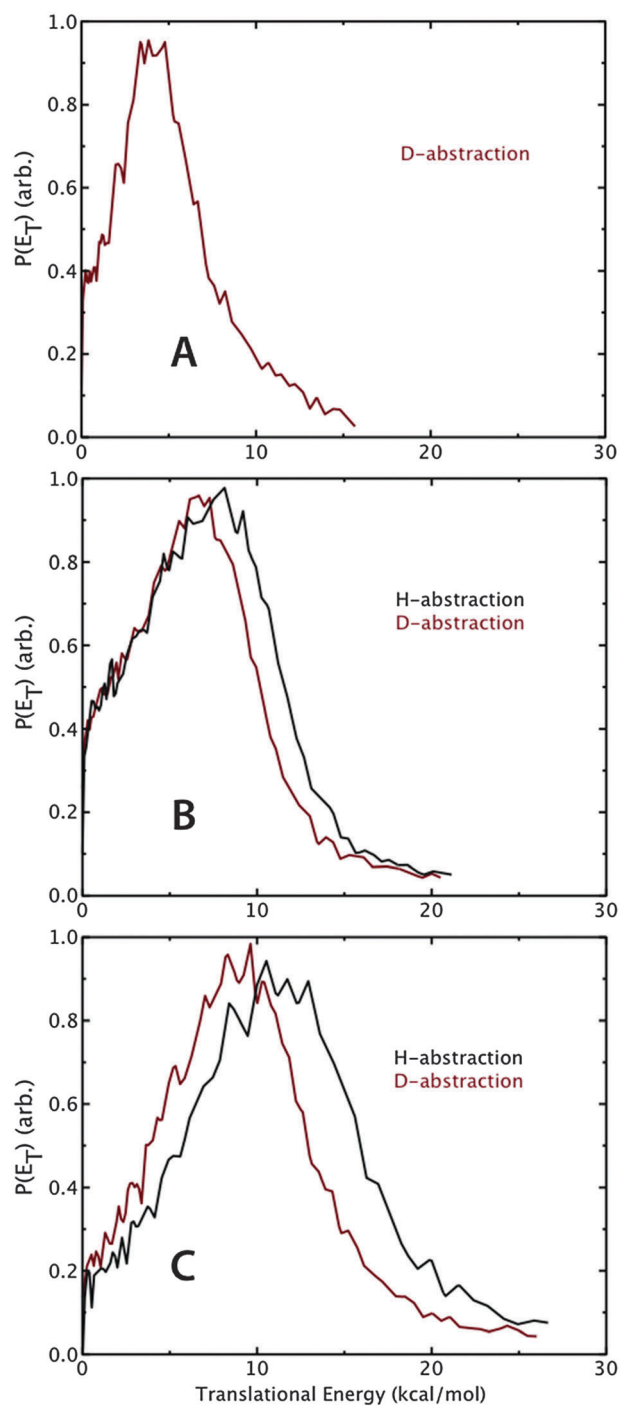


Fig. 2 Total translational energy distributions from data in Fig. 1. (a) D-abstraction at 5.2 kcal mol⁻¹ collision energy; (b) H-abstraction (black curve) and D-abstraction (red curve) at ~10.0 kcal mol⁻¹; (c) H-abstraction (black curve) and D-abstraction (red curve) at ~13.0 kcal mol⁻¹.

in our previous reports.^{23,24} The latter correction is modest, but one significant challenge often associated with the use of 157 nm probe in crossed-beam imaging is a large photochemical background in the forward scattered portion of the image arising from photodissociation of the parent hydrocarbon. This issue has been mitigated in our present configuration with an intense source of Cl radical, and we are able to obtain accurate reactive signals for the full range of scattering except within 5–10° of the hydrocarbon beam.

The total translational energy distributions, integrated over all angles, are given in Fig. 2. The translational energy distributions of the butyl radical products due to H-atom abstraction ($m/z = 63$) peak at higher translational energy than that of D-abstraction ($m/z = 62$) at comparable collision energy of ~ 10 kcal mol $^{-1}$. At ~ 13 kcal mol $^{-1}$ this difference is even more pronounced. Fig. 3 shows the center-of-mass angular distributions, integrated over all recoil directions, derived from the images. The butane beam defines the forward direction (0°). The angular distributions at low collision energy show flux in all directions, with modestly enhanced scattering in the forward direction. As the collision energy increases, the scattering for both the H- and D-atom abstraction shifts to the forward direction for all cases while the backward scattering is reduced. The angular distributions for both channels are remarkably similar.

The average energy release data for the two abstraction channels at each collision energy is compiled in Table 1. For D-abstraction, the fraction of energy appearing in translation is $\sim 65\%$ but is consistently lower for H-abstraction. To gain further insight into the dynamics of the two abstraction channels, we look at the product translational energy distribution in two ways. First, we compare the H and D abstraction channel at comparable collision energies for the forward (10°–60°), sideways (60°–120°), and backward (120°–180°) scattered products, by integrating the signals separately in each portion of the image. These are plotted in Fig. 4. For these heavy-light-heavy systems, it is well known that the kinematics favor conservation of translational energy in the reaction.^{37,38} We have thus found it revealing in our earlier studies to plot the translational energy distributions scaled by the collision energy. This allows dynamical deviations from the dominant kinematic trend to be seen more clearly. The scaled translational energy distributions for each of the two channels separately are shown in Fig. 5 and the average values compiled in Table 2.

Discussion

The most direct study comparable to ours is that of Varley and Dagdigian^{17,18} on the reaction of chlorine atoms with propane deuterated at the secondary site, and isobutane deuterated at the tertiary site. Both systems showed cold DCI and HCl rotational distribution, similar to the distributions of Cl reactions with several small hydrocarbon molecules.⁹ They reported the angular distributions to be mainly backward for DCI and sideways for HCl; however they faced a number of challenges in their studies, including a broad collision energy spread, a spread in initial reagent velocities, and the

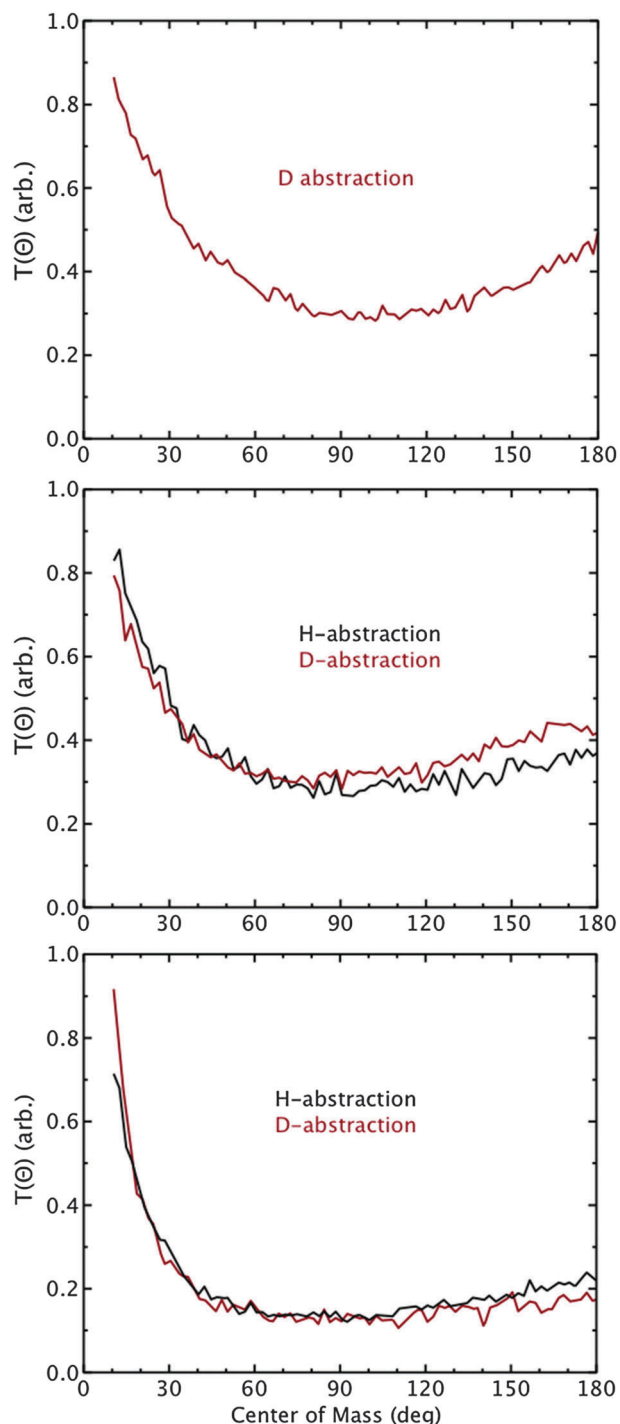


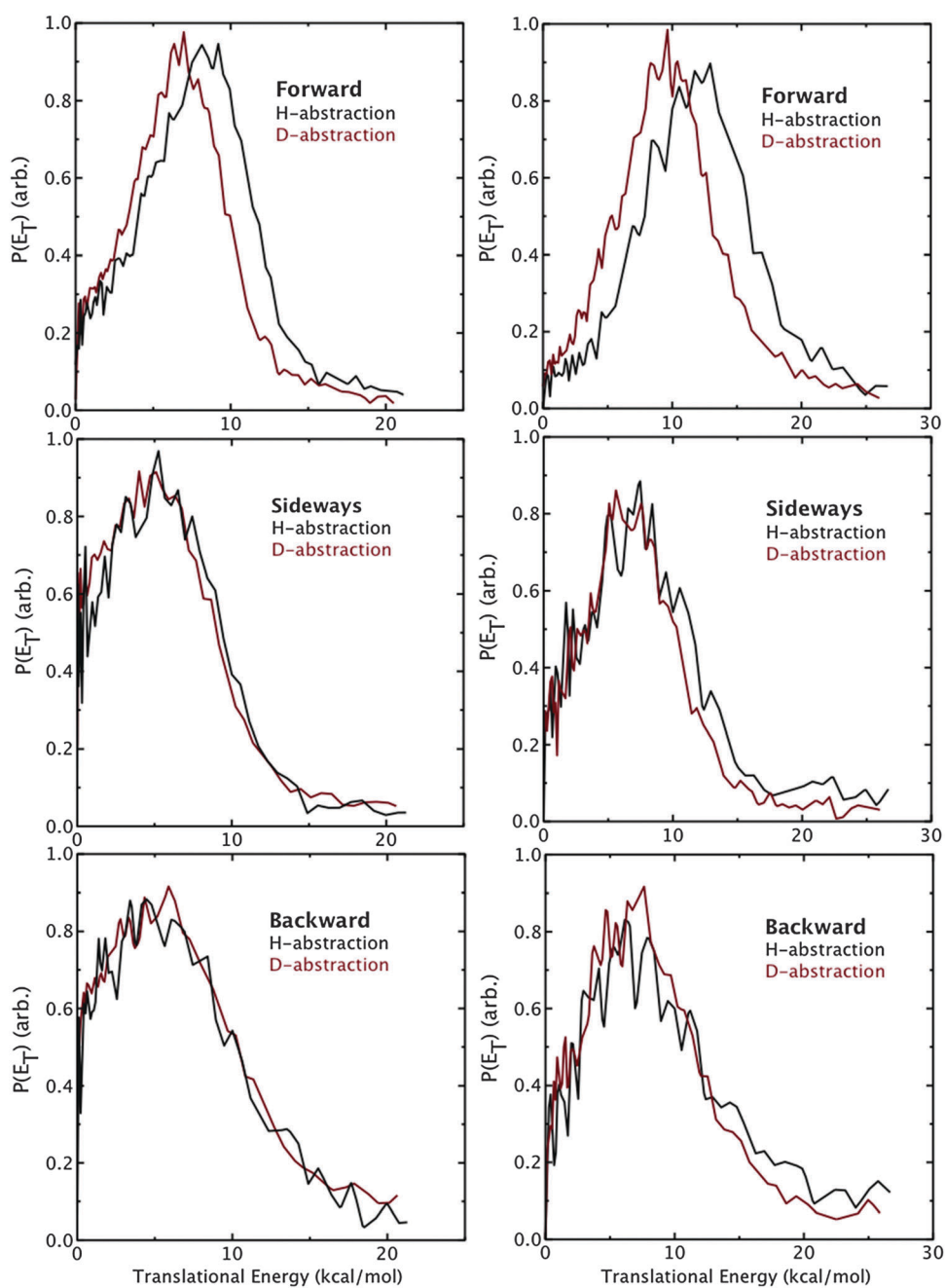
Fig. 3 Total angular distributions from data in Fig. 1. (a) D-abstraction at 5.2 kcal mol $^{-1}$ collision energy; (b) H-abstraction (black curve) and D-abstraction (red curve) at ~ 10.0 kcal mol $^{-1}$; (c) H-abstraction (black curve) and D-abstraction (red curve) at ~ 13.0 kcal mol $^{-1}$.

assumption of a single product recoil velocity was necessary to fit the data.

It is important to note in our study that the D-atoms are attached to primary C atom sites and the H-atom is on the secondary C-atoms. As shown in Fig. 3, at ~ 10.0 kcal mol $^{-1}$ collision energy, the backscattering for the D abstraction is slightly greater than that of the H-abstraction. The difference

Table 1 Collision energy, available energy, average translational energy release, and fraction of available energy appearing in translation

	E_c (kcal mol $^{-1}$)	E_{avail} (kcal mol $^{-1}$)	$\langle E_T \rangle$ total (kcal mol $^{-1}$)	f_t
H-abstraction	10.4	16.4	7.7	0.46
	12.9	18.9	11.2	0.58
D-abstraction	5.2	6.9	4.5	0.65
	9.1	10.8	6.9	0.64
	12.8	14.5	9.0	0.62

**Fig. 4** Center-of-mass translational energy distributions for $\text{Cl}(^2\text{P}_{3/2}) + \text{butane}-1,1,1,4,4-d_6$ reaction and center of mass scattering region: Forward ($10^\circ - 60^\circ$); sideways ($60^\circ - 120^\circ$); backward ($120^\circ - 180^\circ$). Left panel: ~ 10 kcal mol $^{-1}$ collision energy results; right panel: ~ 13 kcal mol $^{-1}$ collision energy results.

however is not very significant. At a collision energy of 7.4 kcal mol $^{-1}$, Bass and coworkers³⁹ studied the nascent $\text{HCl}(v = 0, j)$ from the reaction of Cl atom with n-butane

using photoloc, and reported forward scattering for the abstraction of H at the primary carbon site while abstraction of H atom at the secondary site was seen to be more isotropic

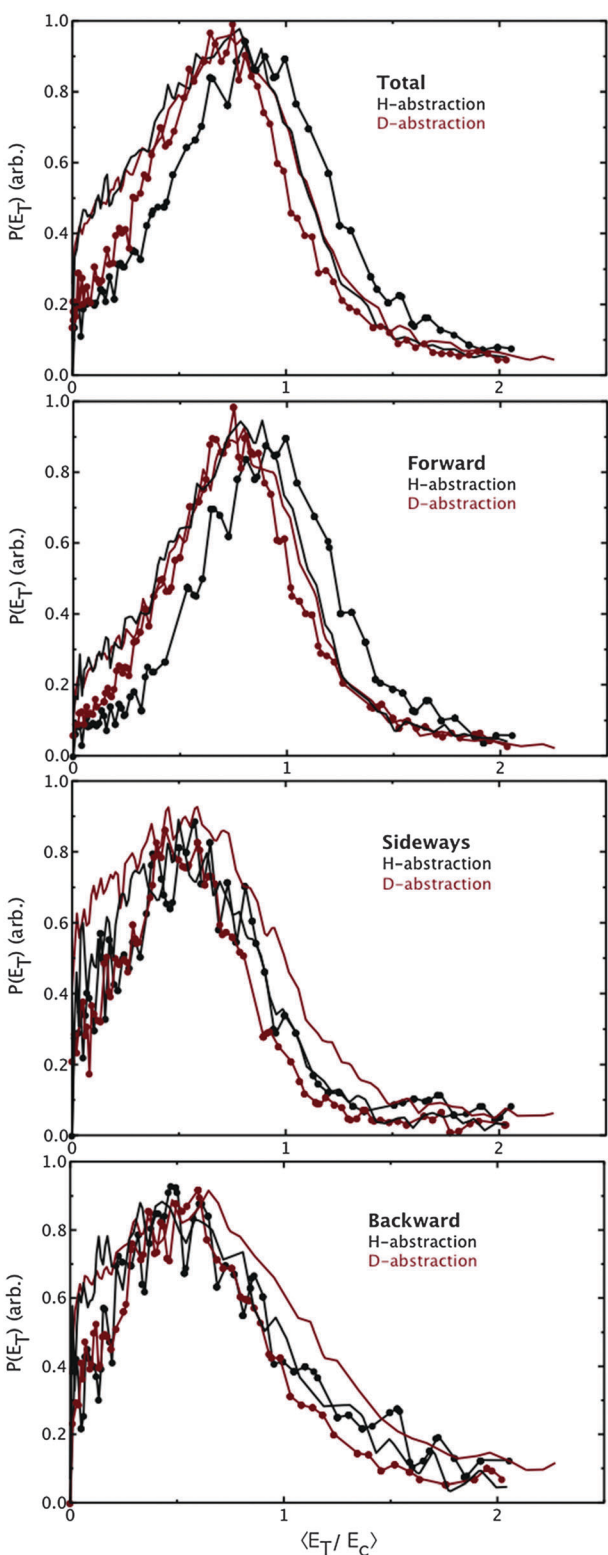


Fig. 5 Reduced translational energy distributions $P(E_T/E_C)$. Red curves are for D-abstraction; solid line: $\sim 10 \text{ kcal mol}^{-1}$ collision energy, dotted line: $\sim 13 \text{ kcal mol}^{-1}$ collision energy. Black curves are for H-abstraction; solid line: $\sim 10 \text{ kcal mol}^{-1}$ collision energy, dotted line: $\sim 13 \text{ kcal mol}^{-1}$ collision energy.

and less forward peaking. This was based on inferences about the energetics for the two channels, and was not a direct probe

of the two channels. However, this experiment was not able to report the full range of the backward distribution owing to the interference of HCl in the beam. Forward-peaking secondary abstraction was argued based on the energy release in crossed-beam studies of Blank *et al.*⁴⁰ and in particular Hemmi and Suits⁴¹ in the reaction of Cl with propane and pentane, respectively. However, the results shown in the present work clearly indicate that the overall scattering angular distributions are surprisingly insensitive to the nature of the H atom site that is the target.

At the highest collision energies studied here, the key feature is the sharp forward peaking, which is essentially identical for both H and D abstraction. Our recent investigation of the Cl + pentane²³ isomers showed a similar tendency toward forward scattering with increasing collision energy, but we did not examine collision energies as high as in the present studies. In relative kinetics studies, Sarzynski and Sztuba showed that abstraction of primary H-atoms suggested a positive activation energy indicating a small barrier towards abstraction, while secondary hydrogen abstraction was barrierless in the reaction of Cl atom with n-butane.¹¹ The sharp forward peaking seen at high energy suggests that large impact parameter collisions show no evidence of this barrier.

Conformational isomerism is an important issue in large molecules in general, and in alkanes in particular. Butane is the simplest hydrocarbon molecule that possesses different conformational minima. The most stable is the *anti* conformation, while a *gauche* conformer lies $0.62 \text{ kcal mol}^{-1}$ higher than the *anti*, and there is a barrier of $3.5 \text{ kcal mol}^{-1}$ separating them.⁴² Under the conditions of our experiment, the *gauche* conformer should be present at a level of $\sim 25\%$ prior to the expansion, and given the high barrier, quenching to the minimum is not likely to occur to any significant extent. So we should bear in mind that roughly one fourth of our alkane target molecules possess a *gauche* geometry. The dynamical consequence of this is not entirely clear, but we can expect the secondary sites to be less stereochemically constrained. We may also expect this to blur the distinction between the primary and secondary dynamics to some extent.

The distinct dynamics for primary vs. secondary abstraction are only clearly manifested in the total translational energy distributions, as shown in Fig. 2 and in the scaled distributions shown in Fig. 5. At collision energy of $\sim 10 \text{ kcal mol}^{-1}$, the translational energy distribution for D-abstraction peaks at slightly lower energy compared to the H-abstraction distribution. The difference is even more pronounced at the highest collision energy of 13 kcal mol^{-1} . This is likely a consequence of the much greater exoergicity for the secondary abstraction reaction, and also the broader range of approach geometries accessible for the barrierless H abstraction. This is also seen in the marked difference of the scaled translational energy of H-abstraction and D-abstraction as a function of scattering region. As seen in Fig. 5 and Table 2, the scaled translational energy release of the D-atom abstraction (red curves) showed strong dependence on collision energy in the backward (120° – 180°) scattered distributions, *i.e.* $\langle E_T \rangle^* = \langle E_T \rangle / E_C = 0.90$ at low collision energy and 0.67 at high collision energy. This suggests that low impact parameter collisions are required to couple the reaction exoergicity into

Table 2 Most probable collision energy, E_c (kcal mol⁻¹); average translational energy release, $\langle E_T \rangle$ (kcal mol⁻¹); average reduced translational energy, $\langle E_T \rangle^* = \langle E_T \rangle / E_c$

	E_c	$\langle E_T \rangle$ total	$\langle E_T \rangle$ fwd	$\langle E_T \rangle$ side	$\langle E_T \rangle$ bwd	$\langle E_T \rangle^*$ total	$\langle E_T \rangle^*$ fwd	$\langle E_T \rangle^*$ side	$\langle E_T \rangle^*$ bwd
H-abstraction	10.4	7.7	8.3	6.6	7.3	0.74	0.79	0.63	0.70
	12.9	11.2	12.1	8.7	9.3	0.86	0.93	0.67	0.72
D-abstraction	9.1	6.9	7.3	6.6	8.2	0.76	0.80	0.73	0.90
	12.8	9.0	10.1	7.6	8.6	0.70	0.79	0.60	0.67

product recoil for the primary abstraction. For the secondary abstraction, we see distinct behavior: in the backward direction there is little change in the scaled translational energy with collision energy, while in the forward direction, there is a larger fraction of the energy in translation as the collision energy increases: $\langle E_T \rangle^*$ rises from 0.79 to 0.93.

The observed average translational energy in the backward directions is about 2/3 of the collision energy except for the D-abstraction at the lowest collision energy where it is ~ 0.90 . To help us explain this we can use the simple kinematic model of Evans *et al.*³⁸ This model predicts the average translational energy release to be given by

$$\langle E_T \rangle = E_C \cos^2 \beta + E_R \sin^2 \beta$$

where β is the skew angle for the reaction, E_C is the collision energy, and E_R is the energy release in the reaction. For heavy-light-heavy reactions, the skew angle is acute^{37,43} such that the second term is negligible. For the deuterium abstraction considered here, $\cos^2 \beta$ is 0.92, while it is 0.96 for hydrogen abstraction. In all cases the observed translational energy release is substantially lower than the values predicted by the kinematic model by Evans *et al.*³⁸ This model is intended for collinear collisions (hence our application to the backscattered product) and in general it works well for three-atom systems. The discrepancy between the predicted average translational energy and the observed energy release is not surprising because the reaction system has a large number of degrees of freedom that are not accounted in this model. Vibration or rotations of the alkyl radical products are two of the factors that are not taken into consideration in this kinematic model. A Franck–Condon picture was invoked by Liu and Suits⁸ in the study of O(³P) with butane. They calculated the relaxation energy of the alkyl from the transition state geometry to be 4–5 kcal mol⁻¹ and argued that this value is not available for recoil of the detected alkyl products. In our case here, there is also likely considerable rotational excitation of the butyl radical products. For the forward scattered products, we see quite similar reduced translational energy release in the forward direction (and below the model prediction), except for primary (D) abstraction at the lower collision energy. We can speculate that these large impact parameter collisions (for forward scattering from primary abstraction) result in little momentum transfer, giving rise to lower rotational excitation in general and a lower likelihood of *A*-axis rotational excitation in particular.

Perhaps the most surprising feature of these results is the absence of any strong signature of the distinct dynamics for these two reaction channels in the angular distributions. It may be that these systems, with little or no barrier and large reaction cross sections, are less sensitive to these issues than

analogous reactions with significant barriers, such as for oxygen atoms. We plan to pursue this question in future investigations.

Conclusions

The abstraction reaction of Cl atom towards butane-1,1,1,4,4,4-*d*₆ has been studied using single-photon ionization using crossed molecular beam dc slice imaging methods. This allowed us to compare in detail the dynamics associated with these two abstraction channels. The angular distributions showed a dramatic increase in the forward scattered product with collision energy for both reaction channels but were very similar for H or D abstraction at all collision energies studied. The translational energy distribution showed some differences for the two channels, with a larger fraction of the collision energy appearing in translation for the H abstraction channel in the forward direction, but an opposite trend for the D abstraction channel.

Acknowledgements

This work was supported by the Director, Office of Science, Office of Basic Energy Science, Division of Chemical Science, Geoscience and Bioscience, of the U.S. Department of Energy under Contract No. DE-FG02-04ER15593.

References

- 1 P. Andresen and A. C. Luntz, *J. Chem. Phys.*, 1980, **72**, 5842.
- 2 A. C. Luntz and P. Andresen, *J. Chem. Phys.*, 1980, **72**, 5851.
- 3 J. H. Park, Y. S. Lee, J. F. Hershberger, J. M. Hossenlopp and G. W. Flynn, *J. Am. Chem. Soc.*, 1992, **114**, 58.
- 4 W. R. Simpson, A. J. Orr-Ewing and R. N. Zare, *Chem. Phys. Lett.*, 1993, **212**, 163.
- 5 W. R. Simpson, A. J. Orr-Ewing, T. P. Rakitzis, S. A. Kandel and R. N. Zare, *J. Chem. Phys.*, 1995, **103**, 7299.
- 6 W. R. Simpson, T. P. Rakitzis, S. A. Kandel, A. J. Orr-Ewing and R. N. Zare, *J. Chem. Phys.*, 1995, **103**, 7313.
- 7 A. J. Orr-Ewing, W. R. Simpson, T. P. Rakitzis, S. A. Kandel and R. N. Zare, *J. Chem. Phys.*, 1997, **106**, 5961.
- 8 X. H. Liu, R. L. Gross, G. E. Hall, J. T. Muckerman and A. G. Suits, *J. Chem. Phys.*, 2002, **117**, 7947.
- 9 C. Murray and A. J. Orr-Ewing, *Int. Rev. Phys. Chem.*, 2004, **23**, 435.
- 10 N. Choi, M. J. Pilling, P. W. Seakins and L. Wang, *Phys. Chem. Chem. Phys.*, 2006, **8**, 2172.
- 11 D. Sarzynski and B. Sztuba, *Int. J. Chem. Kinet.*, 2002, **34**, 651.
- 12 G. S. Tyndall, J. J. Orlando, T. J. Wallington, M. Dill and E. W. Kaiser, *Int. J. Chem. Kinet.*, 1997, **29**, 43.
- 13 T. P. Rakitzis, S. A. Kandel, T. Lev-On and R. N. Zare, *J. Chem. Phys.*, 1997, **107**, 9392.
- 14 D. F. Varley and P. J. Dagdigian, *J. Phys. Chem.*, 1995, **99**, 9843.
- 15 R. A. Rose, S. J. Greaves and A. J. Orr-Ewing, *J. Chem. Phys.*, 2010, **132**, 244312.
- 16 Y. F. Yen, Z. R. Wang, B. Xue and B. Koplitz, *J. Phys. Chem.*, 1994, **98**, 4.

- 17 D. F. Varley and P. J. Dagdigan, *Chem. Phys. Lett.*, 1996, **255**, 393.
- 18 D. F. Varley and P. J. Dagdigan, *J. Phys. Chem.*, 1996, **100**, 4365.
- 19 S. Yan, Y. T. Wu, B. Zhang, X. F. Yue and K. Liu, *Science*, 2007, **316**, 1723.
- 20 M. J. Frisch, G. W. Trucks, H. B. Schlegel, G. E. Scuseria, M. A. Robb, J. R. Cheeseman, G. Scalmani, V. Barone, B. Mennucci, G. A. Petersson, H. Nakatsuji, M. Caricato, X. Li, H. P. Hratchian, A. F. Izmaylov, J. Bloino, G. Zheng, J. L. Sonnenberg, M. Hada, M. Ehara, K. Toyota, R. Fukuda, J. Hasegawa, M. Ishida, T. Nakajima, Y. Honda, O. Kitao, H. Nakai, T. Vreven, J. A. Montgomery, Jr., J. E. Peralta, F. Ogliaro, M. Bearpark, J. J. Heyd, E. Brothers, K. N. Kudin, V. N. Staroverov, R. Kobayashi, J. Normand, K. Raghavachari, A. Rendell, J. C. Burant, S. S. Iyengar, J. Tomasi, M. Cossi, N. Rega, J. M. Millam, M. Klene, J. E. Knox, J. B. Cross, V. Bakken, C. Adamo, J. Jaramillo, R. Gomperts, R. E. Stratmann, O. Yazyev, A. J. Austin, R. Cammi, C. Pomelli, J. Ochterski, R. L. Martin, K. Morokuma, V. G. Zakrzewski, G. A. Voth, P. Salvador, J. J. Dannenberg, S. Dapprich, A. D. Daniels, O. Farkas, J. B. Foresman, J. V. Ortiz, J. Cioslowski and D. J. Fox, *GAUSSIAN 09 (Revision A.1)*, Gaussian, Inc., Wallingford, CT, 2009.
- 21 J. A. Montgomery, M. J. Frisch, J. W. Ochterski and G. A. Petersson, *J. Chem. Phys.*, 1999, **110**, 2822.
- 22 J. A. Montgomery, M. J. Frisch, J. W. Ochterski and G. A. Petersson, *J. Chem. Phys.*, 2000, **112**, 6532.
- 23 A. D. Estillore, L. M. Visger and A. G. Suits, *J. Chem. Phys.*, 2010, **132**, 164313.
- 24 A. D. Estillore, L. M. Visger and A. G. Suits, *J. Chem. Phys.*, 2010, **133**, 074306.
- 25 M. Ahmed, D. S. Peterka and A. G. Suits, *Phys. Chem. Chem. Phys.*, 2000, **2**, 861.
- 26 C. S. Huang, W. Li and A. G. Suits, *J. Chem. Phys.*, 2006, **125**, 133107.
- 27 N. Herath, M. Hause and A. G. Suits, (unpublished results).
- 28 R. Silva, W. Gichuhi, M. Doyle, A. Winney and A. Suits, *Phys. Chem. Chem. Phys.*, 2009, **11**, 4777–4781.
- 29 D. Townsend, M. P. Miniti and A. G. Suits, *Rev. Sci. Instrum.*, 2003, **74**, 2530.
- 30 W. Li, S. D. Chambreau, S. A. Lahankar and A. G. Suits, *Rev. Sci. Instrum.*, 2005, **76**, 63106.
- 31 H. U. Stauffer, R. Z. Hinrichs, P. A. Willis and H. F. Davis, *J. Chem. Phys.*, 1999, **111**, 4101.
- 32 P. A. Willis, H. U. Stauffer, R. Z. Hinrichs and H. F. Davis, *J. Chem. Phys.*, 1998, **108**, 2665.
- 33 M. Ahmed, D. S. Peterka and A. G. Suits, *Chem. Phys. Lett.*, 2000, **317**, 264.
- 34 A. D. Estillore, L. M. Visger, R. I. Kaiser and A. G. Suits, *J. Phys. Chem. Lett.*, 2010, **1**, 2417.
- 35 C. Huang, W. Li, A. D. Estillore and A. G. Suits, *J. Chem. Phys.*, 2008, **129**, 074301.
- 36 X. H. Liu, R. L. Gross and A. G. Suits, *J. Chem. Phys.*, 2002, **116**, 5341.
- 37 C. A. Picconatto, A. Srivastava and J. J. Valentini, *J. Chem. Phys.*, 2001, **114**, 1663.
- 38 G. T. Evans, E. van Kleef and S. Stolte, *J. Chem. Phys.*, 1990, **93**, 4874.
- 39 M. J. Bass, M. Brouard, C. Vallance, T. N. Kitsopoulos, P. C. Samartzis and R. L. Toomes, *J. Chem. Phys.*, 2004, **121**, 7175.
- 40 D. A. Blank, N. Hemmi, A. G. Suits and Y. T. Lee, *Chem. Phys.*, 1998, **231**, 261.
- 41 N. Hemmi and A. G. Suits, *J. Chem. Phys.*, 1998, **109**, 5338.
- 42 N. L. Allinger, J. T. Fermann, W. D. Allen and H. F. Schaefer, *J. Chem. Phys.*, 1997, **106**, 5143.
- 43 A. Teslja and J. J. Valentini, *J. Chem. Phys.*, 2006, **125**, 132304.